Measurement of Spatiotemporal Behavior of Alfvén-Ion-Cyclotron Waves in the GAMMA10 Tandem Mirror*)

Ryuya IKEZOE, Makoto ICHIMURA, Tatsunori SATO, Yasutaka IMAI, Tatsuya MURAKAMI, Toru IWAI, Yumeto UGAJIN, Takuro YOKOYAMA, Yoriko SHIMA, Masayuki YOSHIKAWA and Tsuyoshi IMAI

Plasma Research Center, University of Tsukuba, Tsukuba 305-8577, Japan

(Received 7 December 2010 / Accepted 15 April 2011)

Spatiotemporal behavior of Alfvén-ion-cyclotron (AIC) waves excited in GAMMA10 is investigated using a microwave reflectometer and magnetic probes located at the edge. The frequency spectrum of the AIC waves has several discrete peaks. Simultaneous measurement of the internal density fluctuation and edge magnetic fluctuation of AIC waves shows that AIC waves have different radial structures in the initial excitation phase, but in the later steady state, each of them has the same structure in the radial direction. The results indicate that several AIC waves are excited as the same eigenmode in the radial direction.

Keywords: Alfvén-ion-cyclotron, electromagnetic wave, temperature anisotropy, reflectometer, mirror field, GAMMA10

DOI: 10.1585/pfr.6.2402047

1. Introduction

In magnetized plasmas, various types of electromagnetic waves can exist or grow according to their dispersive properties. Most of the dispersion relations for electromagnetic waves have been derived analytically using appropriate approximations in theoretical works. Although these theories successfully explain some observations in astronomical and laboratory plasmas, much unexplained wave-related physics is yet to be explored. Alfvén-ion-cyclotron (AIC) waves are important waves that have not yet been completely understood, especially in a mirror field [1]. AIC waves were derived theoretically in a system having strong temperature anisotropy, defined as the ratio of components perpendicular to the magnetic field line to those parallel ($T_\perp/T_\parallel$), and high plasma pressure [2]. The theoretically predicted driving force of AIC waves is proportional to $\beta(T_\perp/T_\parallel)^2$.

GAMMA10 is the world's largest tandem mirror machine, consisting of a central cell, two anchor cells, and two plug/barrier cells. AIC waves are spontaneously excited in GAMMA10 with a strong temperature anisotropy of greater than 10 and a high beta value of a few percent, which are achieved by strong ion heating perpendicular to the magnetic field lines by ion cyclotron range of frequency (ICRF) heating in a mirror field. The loss cone, an inherent characteristic of a mirror magnetic field, enhance the anisotropy. Although the effect of AIC waves on plasma confinement has been investigated in detail (e.g., [3–6]), the detailed spatial structure and excitation mechanism remain to be clarified. In this paper, we report the spatiotemporal behavior of AIC waves measured with a combination of a reflectometer and magnetic probes.

This paper is organized as follows. The reflectometer system is described in the following section. In Sec. 3, the characteristics of the AIC waves excited in GAMMA10 are explained. The results of investigations of the radial and axial structures are shown in Secs. 4 and 5, respectively. Finally, this paper is summarized in Sec. 6.

2. Experimental Setup

To investigate the three-dimensional (3-D) structure of AIC waves, we need information on the plasma core region at various axial locations where the plasma parameters vary significantly. It has been shown both theoretically and experimentally that AIC waves involve density fluctuations [7, 8]. Figure 1 shows the radial profiles of the cutoff frequency of the O and X modes for typical GAMMA10 density profiles. If we use the 8-18 GHz, ~ 20 dBm output of a frequency-variable yttrium-iron-garnet (YIG) oscillator as the source, we can measure the density fluctuations at all the radial positions in GAMMA10 with a reflectometer. However, the measurable axial position of a reflectometer is determined by the position of the antenna. To obtain axial information about the AIC waves, we have installed horn antennas at several different axial locations.

We developed the homodyne reflectometer shown in Fig. 2. In this system, a pyramidal horn is used as both transmitter and receiver, which reduces the number of horn antennas that must be installed inside the vacuum chamber.

author's e-mail: ikezoe@prc.tsukuba.ac.jp

*) This article is based on the presentation at the 20th International Toki Conference (ITC20).

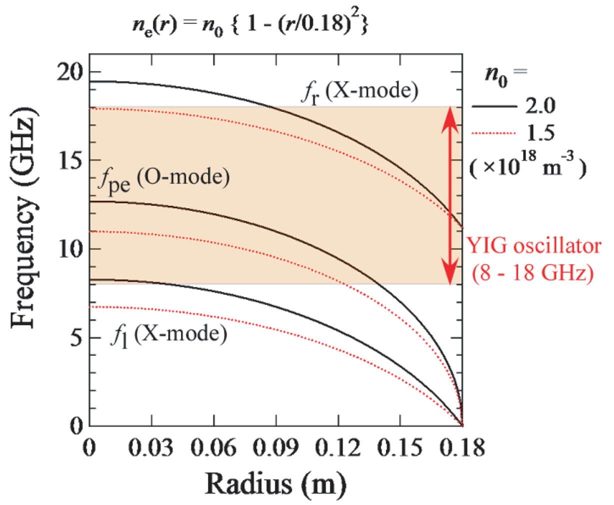

Fig. 1 Radial profiles of cutoff frequency of O and X modes for typical GAMMA10 density profiles.

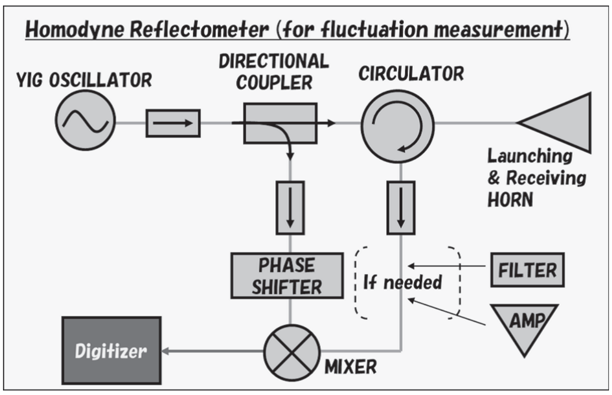

Fig. 2 Schematic of homodyne reflectometer system.

Waves reflected from the plasma are separated from the incident waves by a circulator and mixed with unperturbed local oscillator waves in a mixer. The output of the mixer is expressed as

$$V \approx (a^2 + b^2)/2 + ab\cos\phi$$
$$\approx (a^2 + b^2)/2 + ab(\cos\phi_0 - \delta\phi\sin\phi_0), \qquad (1)$$

where a and b are the amplitudes of the reference and reflected waves, respectively, and ϕ is the phase difference between the reference and reflected waves. Here, ϕ is expressed as the sum of a fixed and/or slow component ϕ_0 and a fast component $\delta\phi$, $\delta\phi \ll \phi_0$. ϕ_0 arises from the difference in the optical path length and the gradual variation in the density profile, and $\delta\phi$ involves other high-frequency components, which are mainly density fluctuations around the reflection point. Since the high-frequency component of the output is proportional to $\delta\phi$, we can extract information about the relevant density fluctuations by calculating the appropriate frequency components.

In this paper, we present the results obtained by using an O-mode horn antenna located at $z = 1.08$ m. The reflectometer is operated at a fixed frequency in a discharge.

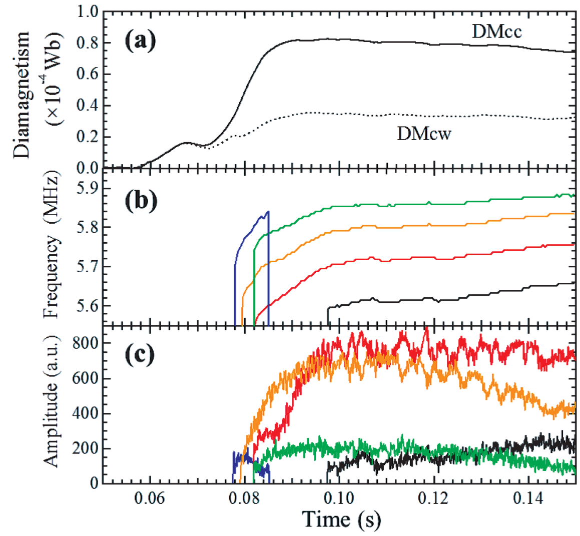

Fig. 3 Temporal evolution of (a) diamagnetism at $z = -0.3$ m, DM_{cc}, and $z = 1.5$ m, DM_{cw}, and (b) frequency and (c) amplitude of AIC waves measured with the edge magnetic probe at $z = 0.82$ m. Colors used in (b) correspond to those used in (c).

3. Temporal Behavior of AIC Waves

In GAMMA10, AIC waves are spontaneously excited when the driving force $\beta(T_\perp/T_\parallel)^2$ exceeds a threshold value, which is well below the theoretical prediction [9]. Figure 3 (a) shows the temporal evolution of the diamagnetism measured near (DM_{cc}) and 1.5 m away from (DM_{cw}) the midplane of the central cell. Diamagnetism is used as an indicator of T_i since $T_i \gg T_e$ for the GAMMA10 plasma. Diamagnetism increases rapidly in the initial plasma production and heating phase with ICRF and saturates below 1×10^{-4} Wb. Since the diamagnetism decreases rapidly in the axial direction, as shown in Fig. 3 (a), the maximum plasma parameters are attained in the narrow central region of the central cell, so AIC waves are expected to be excited near the midplane in the initial excitation phase.

Figure 3 (b) shows the temporal evolution of the peak frequencies in the frequency spectrum of the edge magnetic fluctuation, and Fig. 3 (c) shows the temporal evolution of the amplitude of these components. The five peaks correspond to the five AIC waves. The existence of several waves is typical of AIC waves observed in GAMMA10 and has not yet been explained theoretically. Figure 3 shows that the AIC waves are excited as the diamagnetism increased, and their frequencies and amplitudes vary with the plasma parameters; the number of AIC waves also changes, as shown in Figs. 3 (b) and 3 (c).

4. Radial Structure of AIC Waves

Figure 4 compares the temporal evolution of the frequency spectrum of the edge magnetic fluctuation and the inner density fluctuation measured with a reflectometer us-

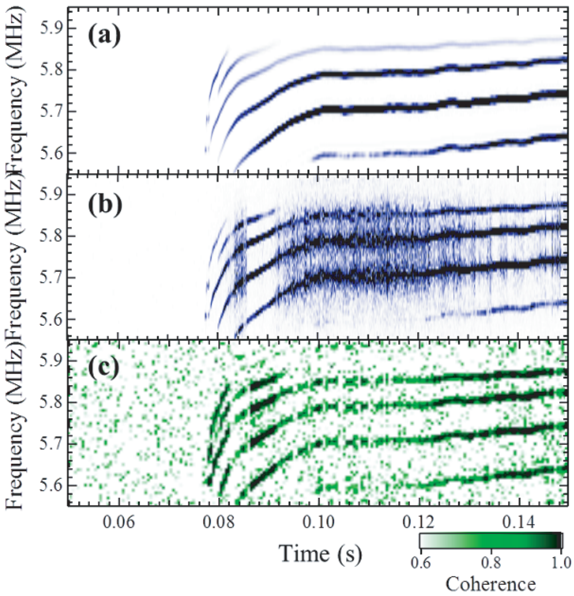

Fig. 4 Temporal evolution of the frequency power spectra of (a) the edge magnetic fluctuation and (b) the inner density fluctuation, and (c) the coherence between the two fluctuations. Dark region denotes high fluctuation power in Figs. 4 (a) and 4 (b).

ing the 10-GHz O mode, the cutoff position of which is approximately r/a = 0.6. Similar temporal behavior can be seen in both spectra except for the clarity of the peaks. Figure 4 (c) shows the coherence between the edge magnetic fluctuation and the inner density fluctuation. When calculating the coherence, we used five ensembles of ~ 164 µs (20 ns $\times 2^{13}$) duration, assuming a steady state of ~1 ms after every 0.5 ms of discharge. Figure 4 (c) clearly shows the temporal evolution of high- coherence branches associated with AIC waves. The coherence tends to decrease when the peaks of the density fluctuation become unclear. Some intense fluctuations such as drift instabilities may affect the clarity of AIC waves measured with the reflectometer.

Since a strong correlation between the two types of fluctuation has been confirmed, as shown in Fig. 4 (c), we can evaluate the phase difference between them. We have surveyed the measurement position of the density fluctuation with the magnetic fluctuation measurement at the same location for reference in a series of discharges in which all the discharge parameters were fixed. We monitored the reproducibility by examining the temporal behavior of the diamagnetism signal.

Figure 5 shows the radial variations in the phase differences between the inner density fluctuation and the edge magnetic fluctuation used as a reference at three different times. Although the horizontal axis represents the incident frequency of the microwaves used, it is associated with the radial profile because the cutoff radius, which is the density fluctuation measurement position, is monotonically related to the incident frequency, as shown in Fig. 1. The left and right sides of the horizontal axis correspond to the core and the edge region, respectively.

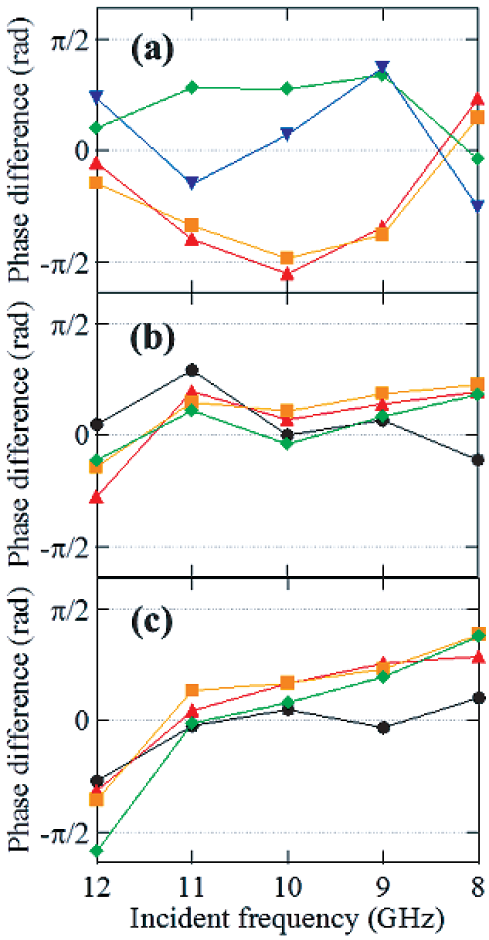

Fig. 5 Radial variation in the phase difference between the inner density fluctuation and edge magnetic fluctuation. Each plot is time averaged over (a) 81.5-85.5 ms, (b) 105-115 ms, and (c) 130-140 ms. Colors correspond to those used in Fig. 3.

The reference magnetic fluctuation was measured at z = 1.12 m, which is close to the position of the horn antenna at z = 1.08 m. In the azimuthal direction, they are separated by 135 degrees. Therefore, the difference in the phase differences at different radial positions indicates the variation in the radial wavelength if the azimuthal wavelength does not change with the radial position. Below, we compare the phase differences in the case of five different incident frequencies. The validity of this type of analysis is based on the assumption of good reproducibility.

Figure 5 (a) shows that in the initial excitation phase, the radial profiles of AIC waves differ except for the two peaks denoted by red and yellow lines, which have larger amplitudes than the others. In the later phase, shown in Figs. 5 (b) and 5 (c), the differences between the peaks are diminished, and those radial profiles approach each other. This behavior indicates that several AIC waves grow as parts of the same structure in the radial direction.

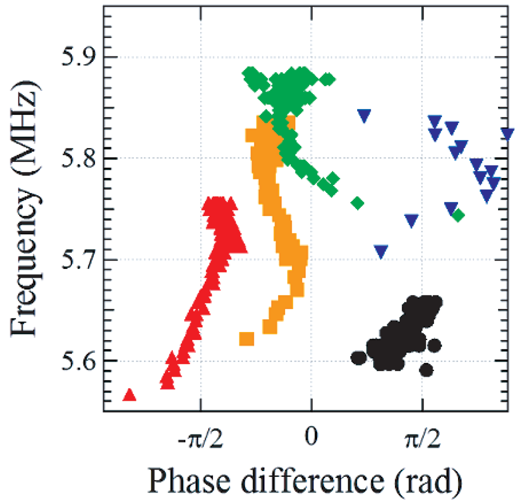

Fig. 6 Frequency vs phase difference for edge magnetic fluctuations at z = 0.82 m and z = 0.98 m, which are separated by 0.16 m in the axial direction.

5. Axial Structure of AIC Waves

We have installed a set of adjacent magnetic probes spaced 0.16 m apart in the axial direction at the edge around $z = 0.9$ m. For discharges similar to those described in Sec. 4, we simultaneously measured two edge magnetic fluctuations with that probe set. The result is shown in Fig. 6 in frequency f and phase difference ϕ space. Although each peak moves in $f - \phi$ space as the plasma parameters vary, each peak gradually settles at a different location as the plasma approaches the steady state. Except for the peak denoted by blue downward triangles, which disappears before the plasma reaches the steady state, each peak has a phase difference of $-\pi/2$ to $\pi/2$. The lowest-frequency peak, denoted by the black circles, propagates in the opposite direction to the others. The other three peaks propagate from the midplane to the end of the central cell, and those wavenumbers are in the range of 0-10 m^{-1} for wavelengths of > 0.6 m. We have clarified that each peak has a different axial structure.

6. Summary

We developed a reflectometer to investigate the detailed 3-D structure of AIC waves excited spontaneously in GAMMA10. The frequency spectrum of the observed AIC waves has several discrete peaks, and the frequency of the peaks and the number of peaks change with the plasma parameters. Simultaneous measurement of the inner density fluctuation by a reflectometer and the edge magnetic fluctuation by a magnetic probe located at almost the same axial location has successfully revealed the radial profile of the AIC waves; each peak has a different radial structure in the initial excitation phase, but in the later steady state, they all have the same structure in the radial direction. This indicates that the observed AIC waves are excited as the same eigenmode in the radial direction.

An adjacent set of magnetic probes spaced in the axial direction revealed that those peaks also have different axial wavenumbers in the steady state in the peripheral region. To investigate the axial structure of the AIC waves, it is important to evaluate the axial wavenumber in the inner plasma region. We have installed horn antennas other than those shown in this paper. In future, we plan to use the reflectometer system with those antennas, which is expected to clarify the detailed 3-D structure of the AIC waves.

Acknowledgments

This work was supported in part by a Grant-in-Aid for Scientific Research from the Ministry of Education, Culture, Sports, Science and Technology of Japan (No. 21540506) and in part by the NIFS Collaborative Research Program (NIFS09KUGM040).

[1] M. Ichimura, J. Plasma Fusion Res. **79**, 5 (2003).
[2] G.R. Smith, Phys. Fluids **27**, 1499 (1984).
[3] M. Nakamura *et al.*, Rev. Sci. Instrum. **72**, 394 (2001).
[4] R. Katsumata *et al.*, Phys. Plasmas **3**, 4489 (1996).
[5] T. Saito *et al.*, Phys. Rev. Lett. **82**, 1169 (1999).
[6] K. Ishii *et al.*, Phys. Plasmas **83**, 3438 (1999).
[7] H. Hojo *et al.*, J. Plasma Fusion Res. **69**, 1043 (1993).
[8] A. Mase *et al.*, Phys. Fluids B **5**, 1677 (1993).
[9] M. Ichimura *et al.*, Phys. Rev. Lett. **70**, 2734 (1993).